American Journal of Materials Science 2024, 14(2): 21-30
DOI: 10.5923/j.materials.20241402.01

Structural and Optical Properties of ZnO:Al:Ga Co-Doped Nanoparticles: Investigation on the Effects of pH of the Precursor Solution via a Simple Sol-Gel Route

Kiprotich Bett[1], Sharon Kiprotich[1,*], Jatani Ungula[2], Warren Andayi[1]

[1]Department of Physical and Biological Sciences, Murang'a University of Technology, Murang'a, Kenya
[2]Department of Applied Sciences, Kenya Methodist University, Meru, Kenya

Abstract Zinc oxide (ZnO) has unique properties that are suitable for solar cell applications. However, there is need to improve its effectiveness by incorporating dopants into ZnO structure. This study investigates how pH affects the material characteristics of ZnO:Al:Ga co-doped nanoparticles Nps) with the goal of maximizing their application in solar cell technology. After the nanoparticles were synthesized using the sol-gel process at different pH values, their optical, morphological, and structural characteristics were analyzed using various techniques. The observed wurtize crystalline structure of ZnO:Al:Ga Nps was validated by X-ray diffraction (XRD) analysis, with the crystallite size estimated to be ranging from 18.83 to 20.94 nm for pH values 7 to 13. The XRD pattern of the as-prepared ZnO:Al:Ga Nps matched well with the Wurtize ZnO crystal structure with variation in peak intensities observed. Scanning electron microscopy (SEM) displayed aggregation of nanoparticles when the precursor pH increased from 7 to 13. The produced ZnO:Al:Ga Nps showed absorption peaks varying from 380 – 376 nm for precursor pH values 7 – 13, with band gap energy range of 3.26 – 3.29 eV as determined from the UV-Vis analysis. Decreased transmittance was observed with the higher pH values of 11–13 due to its larger particles or aggregation tendencies. In addition, chemical bonds and functional groups were examined using Fourier-transform infrared spectroscopy (FTIR). The results confirmed formation of ZnO:Al:Ga Nps as seen in the FTIR peaks corresponding to Zn-O, Al-O, and Ga-O stretching modes between 400 and 590 cm^{-1}. Additionally, the presence of OH stretching bands above the 3000 cm^{-1} region indicates surface hydroxylation.

Keywords Co-doping, ZnO:Al:Ga nanoparticles, Structural properties, Band-gap, FTIR

1. Introduction

Solar energy is leading source of energy for addressing global climate changes due to its reliance on unfriendly energy sources and meeting the world's energy demands for rapidly increasing population growth. In recent years, the search for efficient and sustainable clean energy sources has been intensified as a solution to the negative problems like pollution and the greenhouse effect brought about by the impacts of high dependents on fossil fuels (Huang et al., 2011). The silicon-based solar cells are associated with challenges such as high cost, unreliability, and narrow band gap when it comes to photovoltaic materials. Zinc oxide (ZnO) has attracted a lot of interest due its availability, affordability and unique properties including its ability to be engineered for high efficiency and sustainability of solar energy. The performance of ZnO can be improved by doping with group 13 elements like boron (B) and indium (I) (Bose et al., 2020). However, B and I are not the best dopants because their ionic radii are not as close to Zinc's ionic radius. Aluminum (Al) and Gallium (Ga) are attractive dopants with tailorable properties for high efficiency of ZnO based solar cell applications such as close ionic radii to Zinc, durability, optical transparency, and band-gap tuning (Burunkaya et al., 2010).

Previous studies show that synthesis of ZnO at different pH levels have a significant impact on the properties of nanoparticles. It is well known that strongly alkaline solutions improve the optical and structural properties of nanostructures. For example, Sagar et al. (2007) found that the acidic environment inhibits the formation of ZnO nanostructures. According to Sivakumar et al. (2012), there is an improvement in surface morphology as pH levels rise. This was demonstrated by scanning electron microscopy (SEM) images which showed that at lower pH levels, less uniform grain size distribution was observed but at higher pH levels a distinct and enlarged spherical morphology with self-aligned prismatic nanoparticles is obtained. According

* Corresponding author:
Skiprotich@mut.ac.ke (Sharon Kiprotich)
Received: Apr. 27, 2024; Accepted: May 20, 2024; Published: May 31, 2024
Published online at http://journal.sapub.org/materials

to Alias et al. (2010), ZnO prepared between pH 8 and pH 11 had good optical properties, with the band gap energy (Eg) ranging from 3.14 to 3.25 eV. The synthesis of the nanomaterial under lower pH 7 - 9 conditions resulted in agglomerated particles. ZnO nanoparticles' suitability for solar cell applications can be greatly impacted by the addition of dopants, which can change the material's energy band gap, transmittance, crystallite size, and light absorption (Chand et al., 2012). Furthermore, the parameters of synthesis, such as the pH of the precursor solution, growth temperatures, aging and calcination are critical in defining the final properties of the nanoparticles. Comprehending the impact of pH on the material properties of ZnO:Al:Ga co-doped nanoparticles is crucial in achieving effective high performance solar cells.

The objective of this research is to examine how different pH levels affect the growth of ZnO:Al:Ga nanoparticles for possible solar cell application. The ZnO:Al:Ga co-doped nanoparticles' morphological, structural, and optical properties are all influenced by the synthesis process. The ZnO:Al:Ga co-doped nanoparticles produced by the sol-gel synthesis method were characterized using various techniques to explore the optimum pH of the precursor solution to grow nanoparticles to be incorporated in manufacturing of high performance solar cells.

2. Methodology

Materials

Zinc acetate, aluminum nitrate, gallium nitrate, sodium hydroxide pellets, Ethanol, deionized water. All the chemicals used were of analytical grade and used as purchased without any alteration.

Experimental Procedure

To study the effects of pH of the precursor solution on the material properties of ZnO:Al:Ga co-doped nanoparticles for solar cell applications, ZnO:Al:Ga co-doped nanoparticles were prepared from Zinc acetate dehydrate, Aluminum nitrate, gallium nitrate, sodium hydroxide, ethanol and deionized water. In the beaker, 2.1951 g of zinc acetate was dissolved in 50 mL of ethanol until clear solution was formed, followed by drop wise addition of 25 mL of 1M sodium hydroxide. The precursor solution was kept under constant stirring speed at growth temperature of 75℃. The pH of the precursor solution was varied for the values: 7, 8, 9, 10, 11, 12 and 13 using 5M Hydrochloric acid and 1M Sodium hydroxide. Thereafter, a solution containing 0.187565 g of aluminum nitrate, 0.12787g of gallium nitrate was added to the precursor solution. After one hour the suspension of ZnO:Al:Ga was removed from hot plate and allowed to age. The ZnO:Al:Ga nanoparticles were then washed with deionized water through decantation. The washed samples were dried at 120℃ in the oven and annealed at 600℃. The as-prepared ZnO:Al:Ga co-doped nanoparticles samples were taken for characterization using various techniques: ARL Equinox 100 X-Ray diffractometer (XRD), UV-1800 Shimadzu UV spectrophotometer (UV-Vis), IR spirit Shimadzu Fourier Transform Infrared (FTIR) spectrophotometer, Phenom XLG2 for Scanning Electron Spectroscopy (SEM) and Energy Dispersive X-ray Spectroscopy (EDS).

3. Results and Discussion

XRD Analysis

The XRD analysis of the synthesized ZnO:Al:Ga co-doped nanoparticles is presented in Figure 1, where the diffraction pattern exhibits distinct peaks corresponding to the crystalline phase of hexagonal wurtize present in the sample across all pH values (8, 9, 10, 11, 12, and 13). Wahab et al. (2009) provided similar results, indicating that the diffraction peaks were indexed to the hexagonal wurtzite structure of ZnO that matched with the available Joint Committee on Powder Diffraction Standards for bulk ZnO (JCPDS 36- 1451).

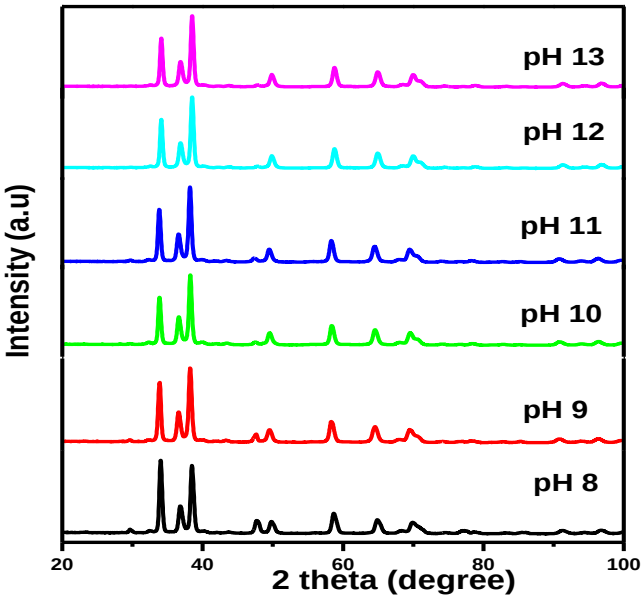

Figure 1. XRD pattern for ZnO:Al:Ga co-doped nanoparticles synthesized at different pH

Figure 1 shows that as pH was varied, no change in crystal phase was observed. No impurity peaks were observed indicating that the synthesized material was of good crystallinity as is confirmed by the reduced full width at half maximum (FWHM) and higher XRD peak intensities of ZnO:Al:Ga Nps as shown by analysis of 101 plane in figure 2.

It can be noted that variation in the FWHM and peak intensities is evident and pH values of the precursor solution is varied. Further analysis was conducted and represented in figure 3. The graph in Figure 3 depicts variations in 2Θ and XRD peak intensity of (101) plane of the corresponding hexagonal wurtize ZnO:Al:Ga codoped nanoparticles. Generally, the diffraction angle 2 theta (degrees) was observed to decrease with increase in pH while the peak intensities increase with increase in pH. The decrease in the

diffraction angle with an increase in pH confirms changes in the nanoparticle standard lattice parameters of ZnO that are brought by imperfections and defects within the material (Seid et al., 2019). The shift to lower diffraction angle could be attributed to increase in the crystallite sizes caused by increase in the lattice parameters as seen in Table 1.

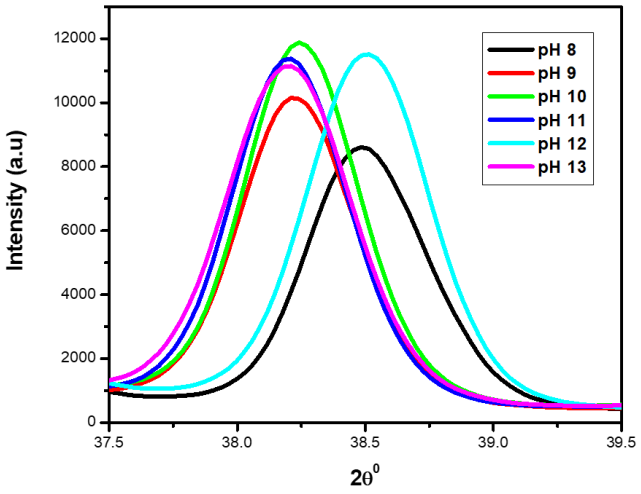

Figure 2. XRD pattern showing magnified (101) peak for the synthesized ZnO:Al:Ga co-doped nanoparticles under varying pH

The crystallite size was calculated using the Scherrer equation $D = \frac{K\lambda}{\beta \cos \theta}$ (Gherbi et al., 2022) where D is crystalline size, K is constant (0.89), λ is 0.154056 nm, mean wavelength of CuKα1 radiation, β is full width half maxima (FWHM) and θ is Bragg's angle in radians. Table 1 shows nano-sized particles with average diameters; 18.69, 19.05, 20.21, 19.52, 19.99 and 19.03 nm for pH values of 8, 9, 10, 12, and 13, respectively. Similar findings were reported by Alias et al. (2010). The sample pH of 8 registered a smallest crystallite size of 18.69 nm while the pH 10 showed the largest crystallite size of 20.21 nm. This is mainly because at pH of 8 the precursor solution is less basic medium whereasat pH of 10, the medium is more alkaline which promotes crystallization (Chen et al., 2020). The size of the ZnO:Al:Ga co-doped crystallites is affected by the size of the FWHM of the XRD peaks. Figure 4 shows the relationship between the crystallite size and the full width at half maximum as pH values of the synthesized ZnO:Al:Ga co-doped nanoparticles are varied. The graph affirmed that crystallite size of nanoparticles are directly proportional to the increase in the pH values on the material properties of the precursor solution while the FWHM decrease with increase in the pH values from 7 – 13. It demonstrates that raising the pH level facilitates the nucleation and development of nanoparticles, the alkaline medium speed up the hydrolysis whereas the acidic medium limits. Alkaline atmosphere promotes hydrolysis when the pH is higher than 7, which increases particle development (Sivakumar et al. (2012) and Jay Chithra et al. (2015).

Table 1. Summary table showing structural parameters of synthesized ZnO:Al:Ga co-doped nanoparticles under varying pH

		pH 8	pH 9	pH 10	pH 11	pH 12	pH 13
2θ	(100)	34.025	33.855	33.860	33.823	34.108	33.823
	D	21.29	20.83	21.68	21.07	22.59	20.26
	(002)	36.869	36.611	36.638	36.600	36.885	36.610
	D	15.95	16.83	18.00	17.03	16.83	16.79
	(101)	38.502	38.230	38.248	38.204	38.507	38.198
	D	18.83	19.48	20.94	20.47	20.56	20.03
	$D_{Average}$	18.69	19.05	20.21	19.52	19.99	19.03
β	(100)	0.39018	0.39844	0.38299	0.39402	0.36772	0.40962
	(002)	0.52492	0.49710	0.46463	0.49129	0.49749	0.49837
	(101)	0.46660	0.45116	0.44502	0.45090	0.47516	0.48724
Peak intensity	(100)	9058.7	8062.7	8329.6	8189.9	8432.5	7632.3
	(002)	3178.1	3787.1	4517.3	4002.8	4061.0	4314.2
	(101)	7908.1	9296.7	10924	10476	10795	10271
δ		0.0029	0.0026	0.0024	0.0026	0.0025	0.0027
∈		0.3324	0.3235	0.3008	0.3080	0.3044	0.3148
Lattice parameters	d	0.2103	0.2117	0.2116	0.2118	0.2102	0.2119
	a=b	0.2698	0.2716	0.2715	0.2718	0.2697	0.2718
	c	0.4908	0.4866	0.4853	0.4856	0.4889	0.4861
Unit volume (V)		0.0315	0.0311	0.0310	0.0311	0.0308	0.0311
$E_g^{Nps} = E_g^{Bulk} + \frac{1.6}{r^2}$		3.39	3.39	3.38	3.38	3.38	3.39

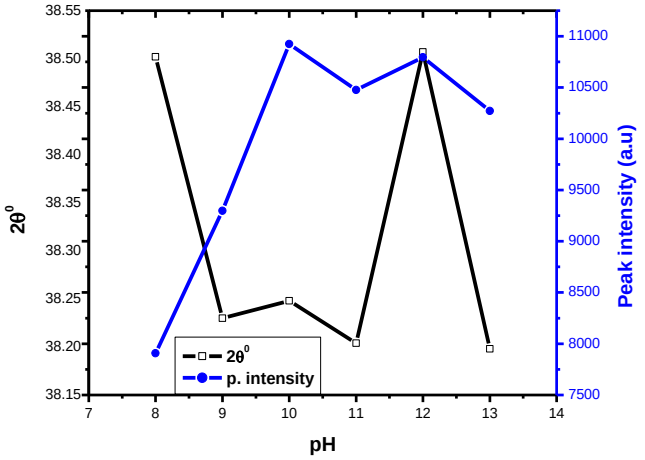

Figure 3. The graph of 2theta and peak intensity verses pH values of ZnO:Al:Ga co-doped nanoparticles synthesized under varying pH

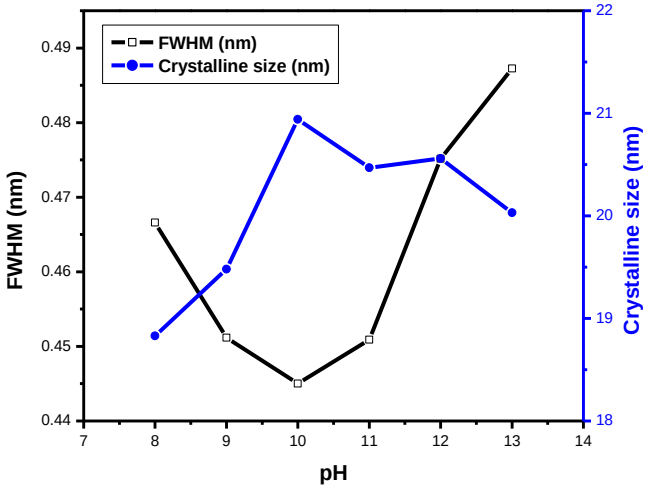

Figure 4. The variation of FWHM and crystallite size (nm) of prepared ZnO:Al:Ga co-doped nanoparticles at different pH

According to Jay Chithra et al. (2015), the XRD peak intensities increased as pH rose, aiding in grain formation and indicating a preference for orientation along the c-axis. The inter-planer, d-spacing was calculated using the Bragg's formula $\lambda=2d\sin\theta$ (Verma et al., 2017), where d is the lattice spacing, θ is the angle of incidence, λ is the wavelength, and n is the diffraction order. The lattice parameters in table 1 were obtained from the equation $\frac{1}{d^2}=\frac{4}{3}\left(\frac{h^2+hk+k^2}{a^2}\right)+\frac{l^2}{c^2}$ (Jay Chithra et al., 2015 &Verma et al., 2017) where 'a' and 'c' are the lattice parameters, h, k, and l are the Miller indices and d is the inter-planer spacing. The prepared ZnO:Al:Ga Nps showed 'a'range from 0.2697 – 0.2718 nm and 'c' to be between 0.4853 – 0.4908 nm. The obtained values confirm the presence of imperfections, defects and strain within the nanoparticles since the values deviated slightly from the values of the ZnO bulk structure.

To find out the dislocation density of the as-prepared Nps, the formula $\delta\frac{1}{D^2}$ (Kiprotich et al., 2022 & Ungula et al., 2024) where δ is the length of dislocation density and D is the crystalline size was utilized. Also, for the micro-strain (∈) values, the equation $\in=\frac{\beta}{4\,tan\theta}$ (Kiprotich et al., 2022) where Θ is the diffraction angle and β is the full width at half maximum (FWHM) were used to find out the cause of the material's imperfections and defects within the structure. The dislocation density and micro-strain values calculated were recorded in table 1. In figure 5, dislocation density and micro-strain are plotted verses pH values. The graph shows that both the micro-strain and dislocation density of the prepared nanoparticles decrease with increase in pH values up to pH = 10 where it starts to rise. This shows that higher pH of the precursor solution promotes formation of defects in the material.

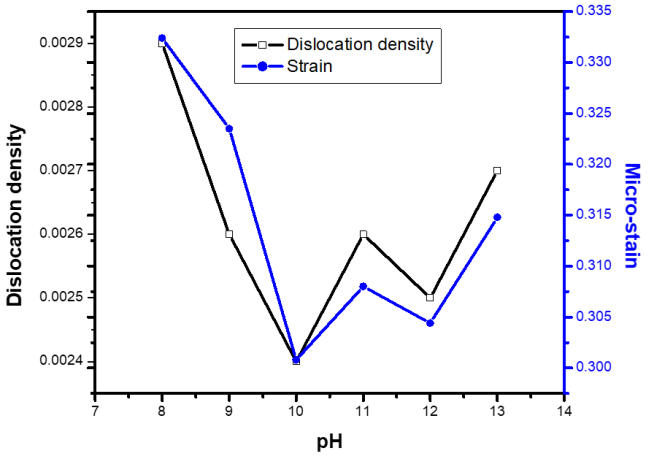

Figure 5. The graph of dislocation density and micro-strain verses pH values of ZnO:Al:Ga co-doped nanoparticles synthesized under varying pH

Additionally, the volume (V) of the unit cell for hexagonal wurtzite structure was calculated by using the equation: $V = 0.866 \times a^2 \times c$ (Chand et al., 2012), and results tabulated in table 1.

The energy band gap can also be calculated using the effective mass model expression from XRD results. The equation is given by; $E_g^{Nps}=E_g^{Bulk}+\frac{1.6}{r^2}$ where E_g^{Nps} is energy band gap of prepared ZnO:Al:Ga co-doped nanoparticles, E_g^{Bulk} is the energy gap of bulk ZnO (3.37 eV) and r is radius of crystal calculated from XRD data results (Jay Chithra et al. (2015)). From the expression the band-gaps values were obtained and recorded in table 1 as follows 3.39, 3.39, 3.38, 3.38, 3.38 and 3.39 eV for the pH values 8 – 13 respectively. From the estimated band gap values, it can be deduced that the energy gaps of the as prepared nanoparticles is inversely proportional to its crystallite radius. This due to the spatial confinement of electrons within the volumes of nanoparticles increases with decreasing crystallite size, leading to discrete energy levels because of quantum confinement (Ramalingam et al., 2020). The nanoparticles' electrical properties are changed by this confinement, specifically their band gap, which is the energy difference between the lowest unoccupied energy level (conduction band) and the highest occupied energy level (valence band). The energy gap between these levels widens as the crystallite size of the nanoparticle decreases due to quantum confinement.

UV-Vis Analysis

Optical properties of the ZnO:Al:Ga co-doped nanoparticles

synthesized under varying pH were obtained from the UV-Vis spectroscopy analysis. Figure 6 displays transmittance spectra with comparable patterns at different pH values. The nanoparticles showed higher transmittance a measure of their degree of transparency to incident light at pH 7. This is attributed by reduced agglomeration at pH 7 which is less alkaline that promotes optimal crystallinity which is uniformly minimizing the presence of defects within the material (Liou & Yang. 2011). This enhanced crystallinity reduces light scattering and absorption, allowing more incident light to pass through the nanoparticles without being hindered hence higher transmittance measure.

On the other hand, transmittance progressively dropped as pH rose, indicating a decrease in light transmission through the nanoparticles. This pattern demonstrated how the optical properties of the nanoparticles are pH-dependent, with pH being a key factor in determining how transparent the particles are to light (Chand et al., 2012).

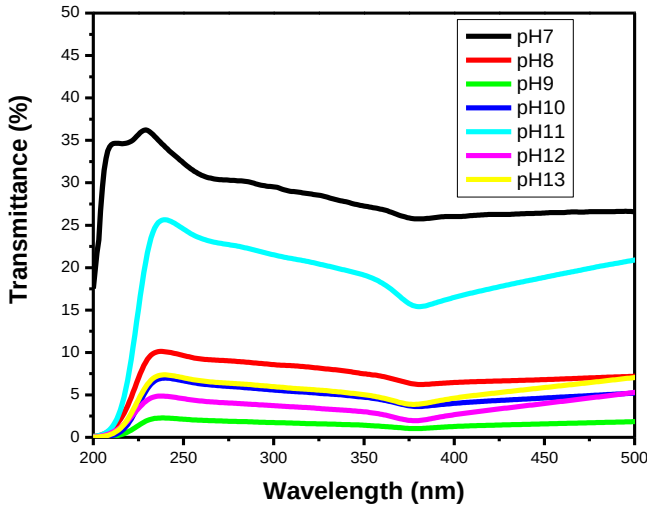

Figure 6. UV-Vis spectrum showing transmittance (%) against wavelength (nm) of as prepared ZnO:Al:Ga co-doped nanoparticles for varying pH values

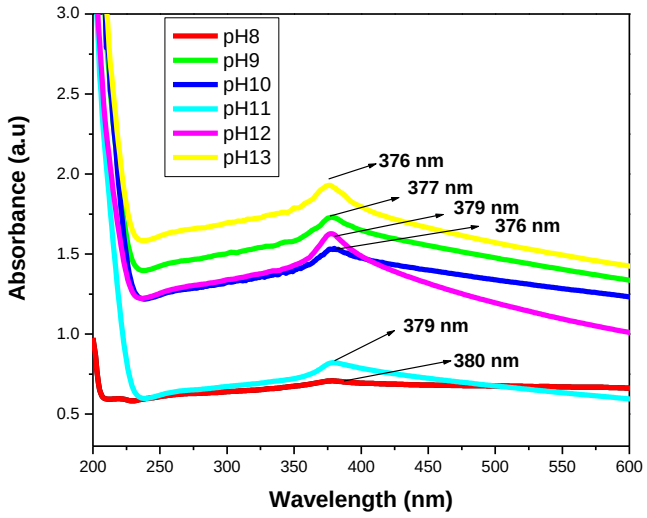

Figure 7. UV-Vis spectrum absorbance (a.u) against wavelength (nm) of ZnO:Al:Ga co-doped nanoparticles with pH values with respective peaks

According to figure 7 and the tabulated data in table 2, the absorbance peaks in the spectra indicated the wavelengths at which the nanoparticles absorbed light approximately to be 376 - 380 nm. This indicates efficient light absorption and corresponds to a band-gap energy of approximately 3.26 – 3.29 eV. A decrease in the band gap energy and electrical structure of the nanoparticles were confirmed by the absorbance peaks shifting towards longer wavelengths with high peak intensity as pH increased.

This is because increasing particle sizes exhibit declining quantum confinement effects, which lower the band gap energy (Smith et al., 2010). The band gap decreases as the energy levels within the nanoparticles go closer together, since the de Broglie wavelength of electrons is no longer limited by the size of the particle. The density and distribution of surface states and defects are also influenced by changes in surface chemistry and morphology, which are brought about by pH variations. The electrical structure of the nanoparticles is directly affected by these surface characteristics changes, which in turn affects the absorption properties of the particles. As a result, as pH rises, the absorbance peaks move towards longer wavelengths at higher intensities. Additionally, the dynamics of charge carriers, such as the processes of creation, recombination, and transport, are impacted by pH-dependent changes in the chemical environment around the nanoparticles. These modifications in charge carrier behavior also affect peak intensity and position in the absorption spectrum. The shifting of absorbance peaks and edges demonstrated how pH influences optical properties of the nanoparticles.

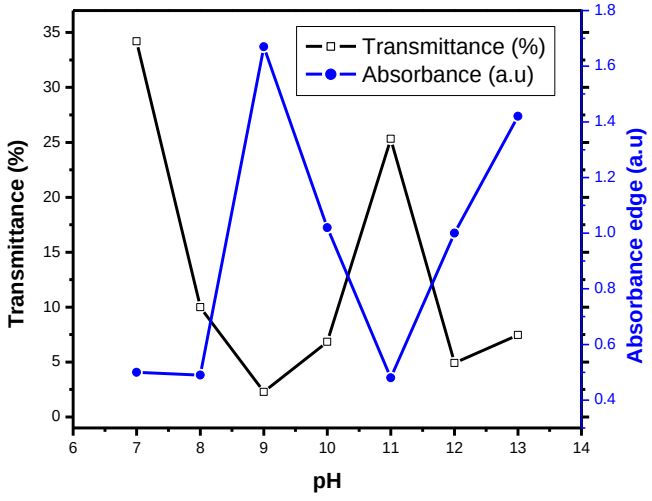

Figure 8. (%) transmittance and absorption edge verses pH values of synthesized ZnO:Al:Ga co-doped nanoparticles with varying pH values

The pH-dependent optical behavior of the ZnO:Al:Ga co-doped nanoparticles is briefly summarized in table 2 & Figure 8, which shows the trends of transmittance (%) and absorbance (in arbitrary units, a.u.) against pH values. The decrease in the transmittance and absorbance at enhanced pH values could be due to defects in the material as confirmed from the XRD results and also by Kara et al., 2020. The sensitivity of ZnO:Al:Ga co-doped nanoparticles' optical

properties to pH changes is emphasized by this graphical representation, which also emphasizes how crucial pH affect optical properties.

By applying Tauc's formula, which reads $(\alpha hv)^2 A(hv - Eg)$ (Ungula et al., 2016) the energy band gap was obtained through extrapolation of the graph of $(\alpha hv)^2$ against $h_{v\,(eV)}$, where A is constant, α is the absorption coefficient (α= 4πk/λ; k is the absorption index), h_v is the photon's energy, Eg is the nanoparticles' energy gap. On the other hand this was estimated theoretically using relationship $E_{bg}=\frac{1240}{\lambda abs}$ which was obtained by;

$$E=hv=\frac{hc}{\lambda}$$

$$\frac{6.625\times10^{-34}Js \times 2.998\times10^{8}m/s}{\lambda(m)}$$

But 1eV $=1.602\times10^{-19}Js$

$$E=\frac{6.625\times10^{-25}Js\ (eV)}{\lambda(m)\times1.602\times10^{-19}Js}$$

But 1nm = $10^{-9}m$

$$E=\frac{1240\ (eV)nm}{\lambda(nm)}$$

From the mathematical equation of a straight line y=mx+c

$$(\alpha hv)^2 A(hv - Eg)$$

Taking y=0, also will be $(\alpha hv)^2 = 0$

$$0= A(hv - Eg)$$

But A=1

Now $hv = Eg$=E

$\therefore E_{bg}=\frac{1240\ (eV)}{\lambda(nm)}$

Therefore, the relation $E_{bg}=\frac{1240}{\lambda abs}$ was used to estimate the energy band-gap of the nanoparticles, and the results showed was 3.27, 3.26, 3.28, 3.28, 3.29, 3.27, 3.29, and 3.29 eV for the samples with pH values of 7, 8, 9, 10, 11, 12, and 13, respectively, as summarized in table 2. These estimated results for energy band-gap matches with the values obtained by Jay Chithra et al. (2015), Verma et al. (2017) & Alias et al. (2010). Perhaps, extrapolation of the Tauc's plot in figure 9 shows different energy band-gaps values that range between 4.6 - 5.8 eV. This is supported by a similar report by Chand et al. (2012) with the result of energy band gap of range 5.57-5.579 eV. This finding highlighted how crucial pH regulation is for adjusting the optical characteristics of the nanoparticles for particular uses, including solar cell devices, where ideal band gap engineering is necessary for effective light absorption and energy conversion. Since pH regulation is essential for tailoring required optical properties of nanoparticles that are suitable for use in solar cells. By precisely controlling the precursors' pH synthesis it tune the band gap that enhance light absorption, stability and durability of the material that improved performance and efficiency of solar cells (Ali et al., 2016).

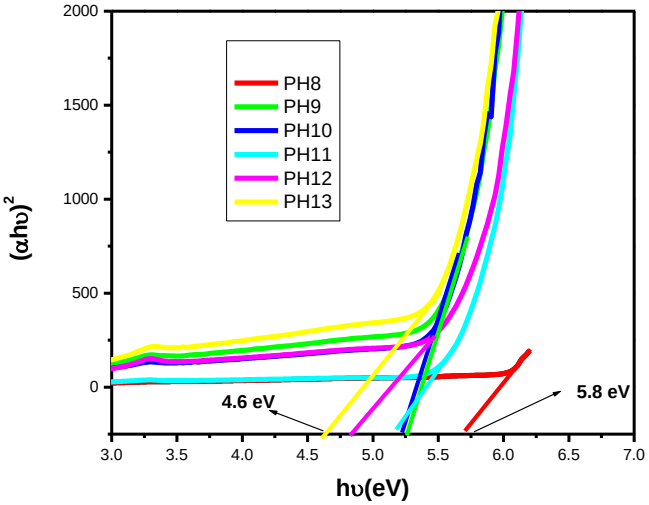

Figure 9. The Tauc's plot for determination of energy band-gaps of synthesized ZnO:Al:Ga co-doped nanoparticles with varying pH values

Furthermore, Table 2 summarizes the data obtained from UV-Vis absorbance spectrum and Tauc's relationship for the prepared ZnO:Al:Ga co-doped nanoparticles under varying pH values. In figure 10, the graph of estimated band-gaps against pH values for synthesized nanoparticles. The findings showed that Tauc's energy band gap of synthesized nanoparticles is inversely proportional to the increase in pH contrary to theoretically energy band gaps and the report done by chad et al. (2012). The inverse relation of the band gap with pH could be due to increase in the crystallite sizes as depicted in the XRD results.

Table 2. Optical data for the as-prepared ZnO:Al:Ga co-doped Nps as the pH is varied

sample	Transmittance (%)	Absorbance edge-gap	λ_{abs}(nm)	$E_{bg}=\frac{1240\ (eV)}{\lambda(nm)}$	Tauc's$E_{bg\,(eV)}$
pH 7	34.2	0.50	379	3.27	5.90
pH 8	10.0	0.49	380	3.26	5.80
pH 9	2.28	1.67	377	3.28	5.30
pH 10	6.85	1.02	376	3.29	5.25
pH 11	25.32	0.48	379	3.27	5.20
pH 12	4.92	1.00	379	3.27	4.80
pH 13	7.46	1.42	376	3.29	4.60

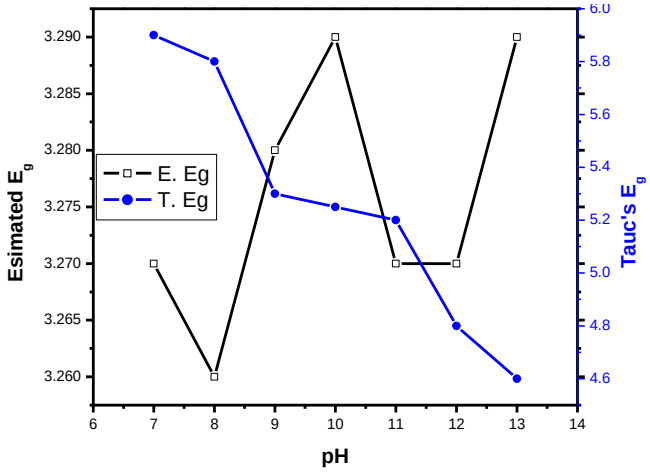

Figure 10. The graph of estimated energy band gaps of prepared ZnO:Al:Ga co-doped nanoparticles

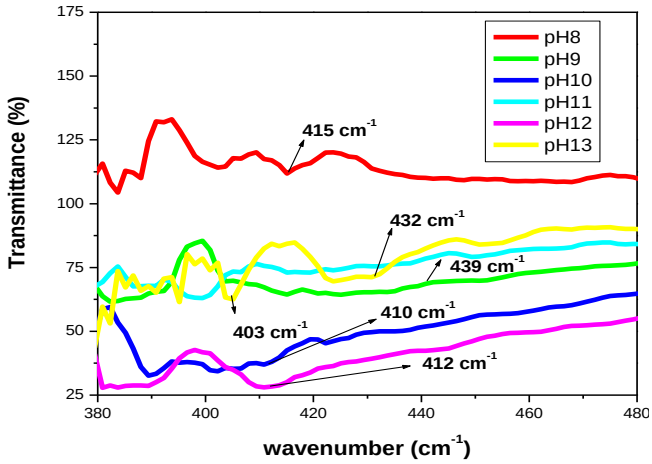

Figure 11. FTIR spectrum % transmittance against wavenumber (cm^{-1}) of ZnO:Al:Ga co-doped nanoparticles with pH values

FTIR Analysis

Significant findings about the ZnO:Al:Ga co-doped nanoparticles' chemical bonding and functional groups were clarified through Fourier-transform infrared spectroscopy (FTIR) analysis. The nanoparticles' vibrational modes and molecular interactions were also revealed by the FTIR spectra, which provided important information about their structural composition. Figure 11 shows that the ZnO:Al:Ga co-doped nanoparticles have different absorption peaks in their FTIR spectra, which correspond to different functional groups. Peaks in the 400–1500 cm^{-1} fingerprint range were indicative of metal–oxygen (M–O) stretching vibrations, which are typical of Zn–O bonds in the crystalline lattice structure of the nanoparticles (Swaroop et al., 2015).

Furthermore, peaks above 3000 cm^{-1} indicated the presence of hydroxyl (OH) groups, which come from adsorbed water molecules or surface hydroxylation (Muharrem et al., 2017). Changes in the FTIR spectra were noted when pH rose from 7 to 13, indicating modifications in the chemical makeup and surface characteristics of the nanoparticles. Peaks corresponding to functional groups, like carboxylates and hydroxyls, expand during synthesis, suggesting alterations in their environment or abundance brought on by pH shifts. Perhaps, as shown in figure 11, the stretching mode peaks at 400 cm-1 are a sign of a successfully synthesized ZnO:Al:Ga nanoparticle. Additionally, shifts in the absorption peaks of systematic pH values of 8, 10, and 12 from 415, 410, and 412 cm^{-1}, respectively, indicate that dopant-oxygen interactions or metal-oxygen bonds occurred, reflecting modifications in the coordination geometry and bonding environment of dopant atoms within the ZnO lattice. These findings offer a true picture of the doping effects of Al and Ga on the chemical structure of the nanoparticles.

SEM Analysis

Using a SEM, the surface morphologies of various samples were determined. With regard to the samples, each image demonstrates the development of a distinct surface morphology. The lamina like-spherical is seen in sample (a) pH 8 in SEM micrographs of figure 12.

Also from figure 12, porous grain-like formations can be observed. ZnO:Al:Ga co-doped nanoparticles synthesized at lower pH levels for example 8, showed a more uniform size distribution on surface. A substantial rise in nanoparticle size and aggregation tendency was seen as the pH level rose from 8 to 12 which are in line with the observations made from the XRD results. According to Jay Chithra et al. (2015), the aggregation phenomena can be explained to be due to the impact of pH on nucleation and growth kinetics during nanoparticle synthesis. The findings of Gherbi et al. (2022), proposed that alkaline medium promote quicker nucleation and growth rates, resulting to larger nanoparticles and these findings are supports the observed rise in nanoparticle size with higher pH values.

Additionally, figure 13 shows energy-dispersive X-ray spectroscopy (EDS) investigation on the elemental composition of pH 12. As shown in table 3, contaminants such as sodium, carbon, and chlorine were found in the nanoparticles in addition to the actual zinc, aluminum and gallium. It is important to carefully manage the synthesis conditions to reduce impurity inclusion, as these impurities may come from precursor compounds or reaction intermediates employed during nanoparticle formation. On the other hand, the Zn and O elements present in the pH 8 nanoparticle EDS micrograph, figure 14 supported the establishment of a pure ZnO composition (Zn- 72.3% and O_2- 27.7%). These results were close to the research done by Hasnidawani. (2016) where the EDX characterization gave Zinc content - 55.38%; Oxygen content - 44.62% with very little impurities observed.

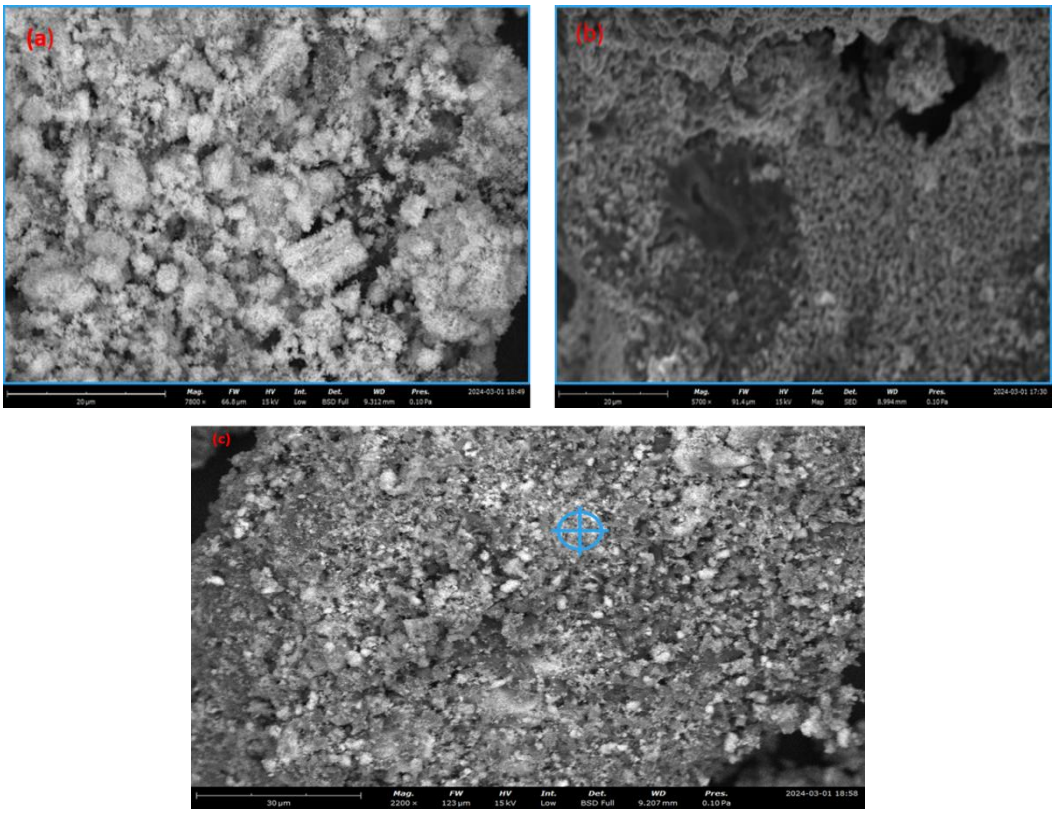

Figure 12. SEM micrographs of synthesized ZnO:Al:Ga co-doped nanoparticles at (a) pH 8 (b) pH 12 (c) pH 10

Table 3. Showing elements of ZnO:Al:Ga sample prepared at pH 12

	Element Number	Element Symbol	Element Name	Atomic Conc.	Weight Conc.
	6	C	Carbon	21.394	11.211
	8	O	Oxygen	44.163	30.831
	11	Na	Sodium	20.448	20.521
	13	Al	Aluminum	0.425	0.501
	17	Cl	Chlorine	1.359	2.102
	30	Zn	Zinc	12.211	34.835

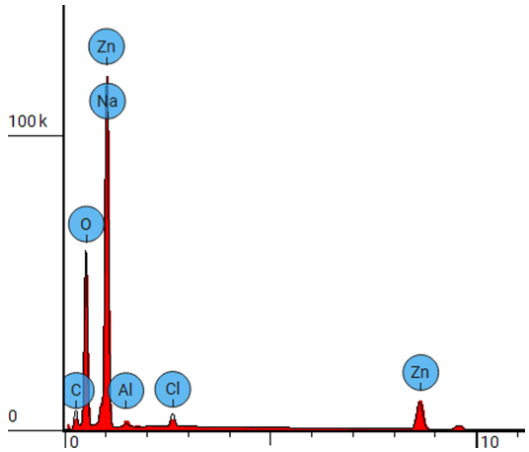

Figure 13. EDS spectrum for ZnO:Al:Ga Nps prepared at pH 12

Theoretically, the expected stoichiometric mass per-cent of Zn and O are 80.3% and 19.7%. as reported by Bari et al., 2009. Table 4 lists the atomic weights and concentrations of the elements Zn and O of the prepared ZnO:Al:Ga co-doped nanoparticles. The observed pH-dependent changes in the morphology and content of nanoparticles point to the possibility of adjusting ZnO:Al:Ga nanoparticles' optical, morphological and structural characteristics for improved solar cell performance.

Table 4. Showing elemental composition of ZnO:Al:Ga Nps sample prepared at pH 8

	Element Number	Element Symbol	Element Name	Atomic Conc.	Weight Conc.
	8	O	Oxygen	61.022	27.700
	30	Zn	Zinc	38.978	72.300

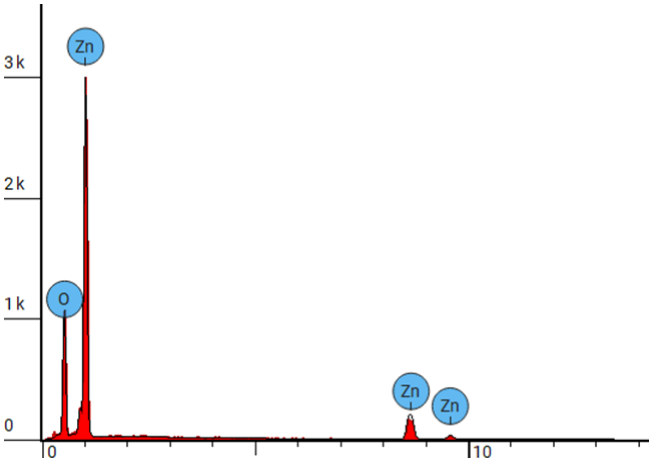

Figure 14. EDS spectrum for ZnO:Al:Ga NPs sample prepared at pH 8

4. Conclusions

ZnO:Al:Ga co-doped nanoparticles were synthesized and characterized under different pH, which have given important understanding into their potential solar cell applications. It was verified by XRD that the dopants were successfully incorporated into ZnO hexagonal wurtize structure. Changes in the optical properties and band-gap energies of the ZnO:Al:Ga nanoparticles were indicated by changes in transmittance and absorbance, as shown by the UV-Vis spectroscopy investigation. Furthermore, SEM established the morphological and elemental composition of the prepared ZnO:Al:Ga co-doped nanoparticles, while Fourier-transform infrared spectroscopy (FTIR) clarified changes in chemical bonding and functional groups, reflecting the influence of pH on the nanoparticles' structural composition. The findings highlighted pH value of 8 as crucial for synthesizing ZnO:Al:Ga co-doped nanoparticles. Greater transparency and narrower band-gap of 4.8 eV were associated with higher pH values, while lower pH levels generally produced wider band-gaps of 5.8 eV and greater transparency as established by Tauc's plot contrary to estimated theoretical energy band-gaps between 3.26 – 3.29 eV. The sol-gel synthesis technique used, was successful means of preparing highly crystalline nanoparticles with crystallite size ranging between 18.69 – 20. 94 nm. These results provide important information for enhancing the synthesis procedure and customizing ZnO:Al:Ga co-doped nanoparticle properties for solar cell application.

ACKNOWLEDGEMENTS

The financial support received from African AI Research grant Award: DSA and Deep Learning Indaba is hereby acknowledged. The authors express gratitude to Murang'a University of Technology for granting access to various synthesis and characterization techniques for the research.

Declaration of Conflict of Interest

There is no conflict of interest to declare by the authors.

REFERENCES

[1] Alias, S. S., Ismail, A. B., & Mohamad, A. A. (2010). Effect of pH on ZnO nanoparticle properties synthesized by sol–gel centrifugation. *Journal of Alloys and Compounds*, *499*(2), 231-237.

[2] Bari, A. R., Shinde, M. D., Deo, V., & Patil, L. A. (2009). Effect of solvents on the particle morphology of nanostructured ZnO.

[3] Bose, S., Mandal, S., Barua, A. K., & Mukhopadhyay, S. (2020). Properties of boron doped ZnO films prepared by reactive sputtering method: Application to amorphous silicon thin film solar cells. Journal of Materials Science & Technology, 55, 136-143.

[4] Burunkaya, E., Kiraz, N., Kesmez, Ö., Erdem Çamurlu, H., Asiltürk, M., & Arpaç, E. (2010). Preparation of aluminum-doped zinc oxide (AZO) nano particles by hydrothermal synthesis. *Journal of sol-gel science and technology*, *55*, 171-176.

[5] Chand, P., Gaur, A., & Kumar, A. (2012). Structural and optical properties of ZnO nanoparticles synthesized at different pH values. *Journal of alloys and compounds*, *539*, 174-178.

[6] Chen, D., Jia, J., Liao, X., Zhou, L., Hu, Z. T., & Pan, B. (2020). Phosphate removal by polystyrene anion exchanger (PsAX)-supporting Fe-loaded nanocomposites: Effects of PsAX functional groups and ferric (hydr) oxide crystallinity. *Chemical Engineering Journal*, *387*, 124193.

[7] Gherbi, B., Laouini, S. E., Meneceur, S., Bouafia, A., Hemmami, H., Tedjani, M. L., ... & Menaa, F. (2022). Effect of pH value on the bandgap energy and particles size for biosynthesis of ZnO nanoparticles: Efficiency for photocatalytic adsorption of methyl orange. *Sustainability*, *14*(18), 11300.

[8] Hasnidawani, J. N., Azlina, H. N., Norita, H., Bonnia, N. N., Ratim, S., & Ali, E. S. (2016). Synthesis of ZnO nanostructures using sol-gel method. *Procedia Chemistry*, *19*, 211-216.

[9] Huang, J., Yin, Z., & Zheng, Q. (2011). Applications of ZnO in organic and hybrid solar cells. Energy & Environmental Science, 4(10), 3861-3877.

[10] Jay Chithra, M., Sathya, M., &Pushpanathan, K. J. A. M. S. (2015). Effect of pH on crystal size and photoluminescence property of ZnO nanoparticles prepared by chemical precipitation method. *ActaMetallurgicaSinica (English Letters)*, *28*, 394-404.

[11] Kara, R., Mentar, L., &Azizi, A. (2020). Synthesis and characterization of Mg-doped ZnO thin-films electrochemically grown on FTO substrates for optoelectronic applications. *RSC advances*, *10*(66), 40467-40479.

[12] Katoch, V., Singh, J., Sharma, N. R., & Singh, R. P. (2021). Synthesis and characterization of mesoporous zinc oxide nanoparticles. *Inorganic and Nano-Metal Chemistry*, 1-9.

[13] Kiprotich, S., Dejene, F. B., &Onani, M. O. (2022). Effects of growth time on the material properties of CdTe/CdSe core/shell nanoparticles prepared by a facile wet chemical route. *Materials Research Express*, *9*(2), 025008.

[14] Liou, T. H., & Yang, C. C. (2011). Synthesis and surface characteristics of nanosilica produced from alkali-extracted rice husk ash. *Materials science and engineering: B*, *176*(7), 521-529.

[15] Muharrem, I. N. C. E., & Ince, O. K. (2017). An overview of adsorption technique for heavy metal removal from water/ wastewater: a critical review. *International Journal of Pure and Applied Sciences*, *3*(2), 10-19.

[16] Ramalingam, G., Kathirgamanathan, P., Ravi, G., Elangovan, T., Manivannan, N., & Kasinathan, K. (2020). Quantum confinement effect of 2D nanomaterials. In *Quantum Dots-Fundamental and Applications*. IntechOpen

[17] Sagar, P., Shishodia, P. K., & Mehra, R. M. (2007). Influence of pH value on the quality of sol–gel derived ZnO films. Applied surface science, 253(12), 5419-5424.

[18] Sakata, K., MinhováMacounová, K., Nebel, R., & Krtil, P. (2020). pH dependent ZnO nanostructures synthesized by hydrothermal approach and surface sensitivity of their photoelectrochemical behavior. *SN Applied Sciences*, *2*, 1-8.

[19] Seid, E. T., Dejene, F. B., & Kroon, R. E. (2019). Synthesis, characterization and influence of pH on indium doped zinc oxide nanostructures. *Ceramics International*, *45*(18), 24269-24278.

[20] Sivakumar, K., Senthil Kumar, V., Muthukumarasamy, N., Thambidurai, M., & Senthil, T. S. (2012). Influence of pH on ZnOnanocrystalline thin films prepared by sol–gel dip coating method. Bulletin of Materials Science, 35(3), 327-331.

[21] Smith, A. M., & Nie, S. (2010). Semiconductor nanocrystals: structure, properties, and band gap engineering. *Accounts of chemical research*, *43*(2), 190-200.

[22] Swaroop, K., & Somashekarappa, H. (2015). Effect of pH values on surface morphology and particle size variation in ZnO nanoparticles synthesised by co-precipitation method. *Research Journal of Recent Sciences*, *2277*, 2502.

[23] Ungula, J., Dejene, F. B., & Swart, H. C. (2016, July). Effects of different Ga doping concentration on structural and optical properties of Ga-doped ZnO nanoparticles by precipitation reflux method. In *Proceedings of the 61st Annual Conference of the South African Institute of Physics, Johannesburg, South Africa* (pp. 4-8).

[24] Ungula, J., Kiprotich, S., & Swart, H. C. (2024). Effect of Deposition Time on Material Properties of ZnONanorods Grown on GZO Seed Layer by CBD. *Journal of Nanosciences Research & Reports. SRC/JNSRR-170. DOI: doi. org/10.473 63/JNSRR/2024 (6)*, *156*, 2-6.

[25] Verma, N., Bhatia, S., &Bedi, R. K. (2017). Role of pH on electrical, optical and photocatalytic properties of ZnO based nanoparticles. *Journal of Materials Science: Materials in Electronics*, *28*(13), 9788-9797.

[26] Wafula, B. J., Masika, E., &Onindo, C. (2020). ZnO Nanoparticles (ZnO-NPs): Synthesis Using Tithoniadiversifolia, Characterization and in-vitro Antimicrobial Bioassays. *J. Appl. Chem. (IOSR-JAC)*, *13*(8), 14-21.

[27] Wahab, R., Kim, Y. S., & Shin, H. S. (2009). Synthesis, characterization and effect of pH variation on zinc oxide nanostructures. *Materials transactions*, *50*(8), 2092-2097.